Studies of J-PET detector to monitor range uncertainty in proton therapy

Baran Jakub, Gajewski Jan, Pawlik-Niedźwiecka Monika, Moskal Paweł, Ruciński Antoni
on behalf of the J-PET Collaboration

Abstract—A problem of range uncertainty is currently one of the most challenging in proton radiotherapy. To tackle that issue, the new, affordable, modular, lightweight, portable and reconfigurable technology of plastic scintillator based positron emission tomography was investigated. Monte Carlo simulation study was performed to evaluate the feasibility of the J-PET technology for proton beam range monitoring. Various configurations (single-layer, multi-layer, full ring, dual-head) were considered. 3D PET images were reconstructed using open-source CASToR software and the expected detector signal, as a function of detector acceptance and efficiency, was estimated. A relationship between the dose and activity profiles was investigated. Experimental validation of the presented results is currently under the preparation.

I. INTRODUCTION

PROTON beam therapy (PBT) is an established cancer radiotherapy technique. Due to the maximum dose deposited in the Bragg peak, at the end of the proton beam range, PBT offers very good conformity of the dose delivered to the target volume allowing to spare the surroundings organs [1]. Currently, in the clinical routine, safety margins around the tumor of 3.5% proton range are applied in order to ensure robust coverage of tumor volume. Potentially, an accurate proton beam range monitoring could decrease the safety margins [2]. Several different techniques, relying on secondary radiation detected during or after the irradiation, were introduced and tested in the clinic. Positron Emission Tomography (PET) [3]–[5], prompt gamma monitoring [6], [7] and secondary charged particles tracking [8]–[10] approaches were investigated. Lastly, the feasibility of time reversal-based protoacoustic reconstruction in 2D for proton range verification was demonstrated using simulations [11]. In case of intra-treatment PBT imaging, distributions of annihilation gammas originating from β^+ emitters produced by energetc protons and acquired in PET scanners could be correlated with the proton beam range. Various clinical setups (in-beam, off-beam or after-treatment PET) could be considered.

The new PET technology is developed at the Jagiellonian University (J-PET), Kraków, Poland. In J-PET inorganic crystals (i.e. LSO, LYSO, BGO) are replaced by the EJ-230 (ELJEN Technology) organic plastic scintillator strips. The energy is deposited in the strips by Compton scattering (not photoelectric absorbtion as in inorganic crystals). Produced light scintillations are propagated throughout the strip up to its end and converted into electric signals. Schematic depiction of the signal acquisition concept with J-PET is presented in Fig. 1. The J-PET prototype consists of 192 strips ($7 \times 19 \times 500\,\mathrm{mm}^3$) assembled to vacuum tube multipliers and arranged into three cylindrical layers enabling acquisition of time-of-flight (TOF) information. Moreover, TOF information is also used to determine the position of energy deposition along the strip length. The scanner is dedicated for fundamental physics studies on positronium imaging in the cancer diagnostic context [12], discrete symmetries investigations [13], [14] and quantum entanglement research [15], [16].

The second generation J-PET scanner (depicted in Fig. 1) is already constructed and tested. Each of the 24 detection modules consist of 13 independent, long scitillator strips ($6 \times 24 \times 500\,\mathrm{mm}^3$). The vaccum tube photomultipliers are replaced by the silicon photomultipliers (SiPM). The signals are susequently read-out by a fast, customized on-board front-end electronics with coincidence resolving time (CRT) of about $500\,\mathrm{ps}$ [17]–[19]. Proposed modular, lightweight and portable design of the scanner allows investigations of various geometrical configurations depending on the application [20]–[22].

The aim of this work is to study the feasibility of the new, plastic scintilator based J-PET technology for range verification in PBT. Number of coincidences for different geometrical configurations, examples of reconstructed images based on Monte Carlo simulations and differences between the dose and reconstructed activity profiles will be presented.

II. MATERIALS AND METHODS

A. Monte Carlo simulations

GATE Monte Carlo toolkit [23] (ver. 8.2) with Geant4 [24] ver. 10.4.2 was used to simulate six geometrical configurations of J-PET modules based on modular J-PET system (single-layer, multi-layer, cylindrical, dual-head). Configurations were selected to address two potential clinic conditions: in-room/off-beam (cylindrical) and in-room/in-beam (dual-head). The simulated number of coincidences acquired
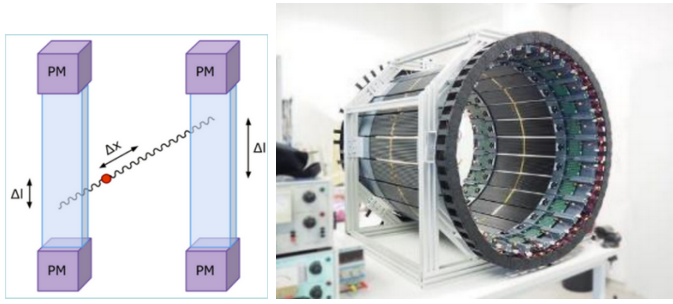
Fig. 1. Scheme of the J-PET concept (left). Modular J-PET scanner. Each of 24 modules consists of 13 scintillating strips (right).

Fig. 3. J-PET geometrical configurations used for single layer barrel (A), double layer barrel (B), triple layer barrel (C), single layer dual-head (D), double layer dual-head (E), triple layer dual-head (F).

with J-PET, originated from β^+ annihilation photons induced in PMMA target (5x5x20cm^3) by a proton beam was investigated (Fig. 2). The PMMA ionization potential was set to 80 eV. The simulated configurations are presented in Fig. 3 and listed in Table I. The configurations (A), (E) and (F) were constructed with the same number of modules to assess if the addition of more layers increases the number of registered coincidence events. 10^8 primary protons (150 MeV) were simulated for each setup. The time structure and physical model of the proton beam applied clinically for cancer patient treatment of the Cyclotron Centre Bronowice (CCB) located in Kraków, Poland was implemented in Monte Carlo simulations as described in [25] and used for the simulations. The QGSP_BIC_HP_EMY physics list was used in simulations with additional RadioactiveDecay model incorporated. The energy and time windows were set on 200-380 keV and 3 ns, respectively. The energy window was set to:
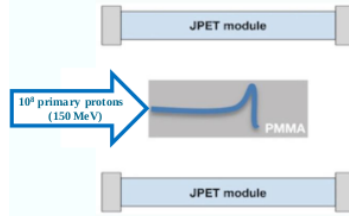

Fig. 2. Schematic view on the simulation setup cross section.

1) Avoid mixing of the signal originating from the charged particle and back-to-back photon interactions with the plastic scintillators, which have energy above this threshold.
2) Decrease the scattered coincidences fraction due to multiple scattering.

GATE PhaseSpace actor was set to obtain the true activity profile.

B. PET data reconstruction

Customizable and Advanced Software for Tomographic Reconstruction (CASToR) [26] ver. 2.0.3 was used for the 3D reconstruction of β^+ activity distributions. Since CASToR does not take into account TOF information on the propagation of scintillation light along the strip, plastic scintillators discretization to 100 digital rings ($7\times19\times5$ mm^3) was applied in axial direction. The list-mode TOF-MLEM reconstruction algorithm (5 iterations with 500 ps TOF resolution without
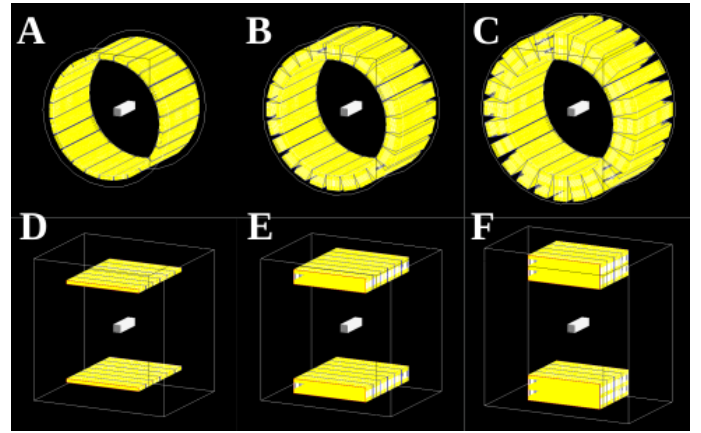
regularization) was used accounting for attenuation and normalization corrections. PMMA linear attenuation coefficient was set to 0.104 cm^{-1}. The activity map was reconstructed in 2.5 mm^3 isotropic voxel grid. All the coincidences (true and scattered) integrated over the time were used in the reconstruction. Scatter and random corrections were not performed. Reconstructed images were smoothed using 3D Gaussian filter with $\sigma = 7.5\times7.5\times7.5$ mm^3 (3x3x3 voxels).

TABLE I
CONFIGURATIONS CHARACTERISTIC AND TOTAL NUMBER OF REGISTERED COINCIDENCES PER 10^8 PRIMARY PROTONS.

CONFIGURATION	NUMBER OF MODULES	GEOMETRICAL ACCEPTANCE	COINCIDENCES		
			ALL	TRUE	SCATTERED
single layer barrel (A)	24	0.39	590	455	94
double layer barrel (B)	48	0.39	1202	943	218
triple layer barrel (C)	72	0.39	1657	1318	285
single layer dual-head (D)	12	0.27	280	231	51
double layer dual-head (E)	24	0.27	948	764	161
triple layer dual-head (F)	24	0.18	1043	871	152

C. Data analysis

The activity profiles were integrated along the beam direction within the whole PMMA phantom region. The sigmoid function was fitted to the distal fall-offs of the activity profiles:

1) Produced in a simulations "true" activity.
2) Actual signal registered with J-PET.

produced in a phantom and reconstructed activity profiles. The sigmoid function is fitted to the produced and reconstructed activity distal fall-offs and the difference between the fall-offs (at the half maximum) was calculated.

III. RESULTS

Table I lists the total number of registered coincidence events integrated over time per 10^8 primary protons. True and scattered fractions are distinguished. The comparison between the geometrical configurations with the same number of modules (A,E and F) revealed that the greater number of layers have the prevailing effect on number of registered coincidences over the geometrical acceptance.
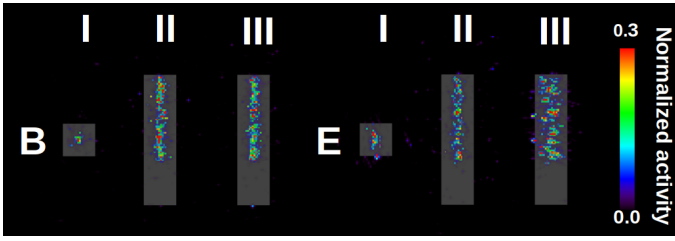
Fig. 4. Normalized reconstructed β^+ activity distributions for the double layer barrel (B) and double layer dual-head (E) configurations in axial (I), coronal (II) and sagittal (III) view. Images were post-smoothed.

An example of the reconstructed PET images superimposed on the CT of the homogeneous PMMA phantom for two geometrical configurations (double layer barrel and dual-head) are presented in Fig. 4. Reconstructed and produced (Monte Carlo) β^+ lateral profiles integrated along Z direction, over the whole phantom region for the double layer barrel and double layer dual-head configurations are presented in Fig. 5.
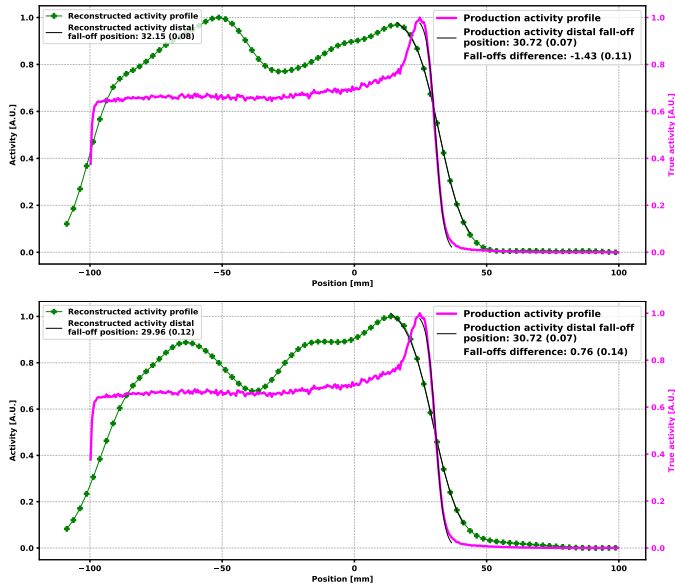

Fig. 5. Normalized reconstructed and true β^+ activity profiles integrated along Z direction over PMMA phantom for: double layer barrel (top) and dual-head (bottom). Phantom area is from -100 mm to 100 mm.

Although the small statistics, all setup configurations enable reconstruction of the β^+ activity produced by proton beams. The calculated differences between the produced and reconstructed profiles are below 2 mm and a good agreement between the profile shapes is observed (Table II). However, the results suggest that presented configurations might overestimate the proton beam range.

IV. CONCLUSIONS

The simulation results show that all presented configurations based on J-PET detector are feasible to acquire the β^+ activity produced by therapeutic proton beams in phantom which are sufficient for 3D reconstruction of PET activity distributions using CASToR. However, iterative reconstruction algorithms

are not optimally suited for the reconstruction of the low statistics PET images acquired with J-PET during proton therapy irradiation. Further investigation with different reconstruction algorithms is needed.

Although, the results show good agreement between the estimated range from the produced and reconstructed activity profiles, it is found that simulations from five configuration setups slightly overestimate the proton beam range, which might be addressed applying calibration, if the absolute activity range is needed. This aspect requires further investigation. Moreover, in order to decrease time needed for simulations, the variance reduction techniques might be employed. Presented results are calculated based on signal measured within the whole PMMA phantom. The region in which the signal is integrated e.g. the center of the PMMA phantom only, has to be also optimized.

Further analysis is needed to correlate the reconstructed β^+ activity profile with the dose distribution distal fall-off. Treatment planning studies are needed to understand if application of the J-PET technology has a potential to decrease the safety margins around the tumor. So far only off-beam setups are considered for the J-PET application for proton beam range verification. For this purpose cylindrical setups are desired due to larger geometrical acceptance, higher statistics and better image quality. For the in-beam scenario, better solution seems to be a dual-head approach as cylindrical J-PET based scanners will override with the moving gantry. However, its application has to be carefully investigated in terms of hardware (how to embedded dual-head J-PET scanner to the moving gantry) and software ('in-fly' PET reconstruction). Solutions developed within the J-PET collaboration utilizing FPGA electronics [18] have a great potential to overcame these difficulties.

The characterization of J-PET sensitivity for proton beam range detection is currently ongoing research activity. The future plans include simulations of β^+ activity induced in patient by proton treatment plans as well as experimental validation of the simulations.

REFERENCES

[1] M. Durante, R. Orecchia, and J. S. Loeffler, "Charged-particle therapy in cancer: clinical uses and future perspectives," *Nature Reviews Clinical Oncology*, vol. 14, pp. 483 EP –, 03 2017. [Online]. Available: http://dx.doi.org/10.1038/nrclinonc.2017.30

[2] H. Paganetti, *Proton Therapy Physics*, J. G. Webster, S. Tabakov, and K.-H. Ng, Eds. Boston, USA: CRC Press Taylor & Francis Group, 2012, vol. 103.

[3] M. G. Bisogni *et al.*, "INSIDE in-beam positron emission tomography system for particle range monitoring in hadrontherapy," *Journal of Medical Imaging*, vol. 4, no. 1, p. 011005, 2016. [Online]. Available: https://doi.org/10.1117/1.JMI.4.1.011005

[4] V. Ferrero, E. Fiorina, M. Morrocchi *et al.*, "Online proton therapy monitoring: clinical test of a Silicon-photodetector-based in-beam PET," *Scientific Reports*, vol. 8, no. 1, p. 4100, 2018. [Online]. Available: http://www.nature.com/articles/s41598-018-22325-6

[5] J. Bauer *et al.*, "Implementation and initial clinical experience of offline PET/CT-based verification of scanned carbon ion treatment," *Radiotherapy and Oncology*, vol. 107, no. 2, pp. 218–226, 2013. [Online]. Available: http://dx.doi.org/10.1016/j.radonc.2013.02.018

[6] J. Krimmer, D. Dauvergne, J. M. Létang, and Testa, "Prompt-gamma monitoring in hadrontherapy: A review," *Nuclear Instruments and Methods in Physics Research, Section A: Accelerators, Spectrometers, Detectors and Associated Equipment*, vol. 878, no. May 2017, pp. 58–73, 2018. [Online]. Available: http://dx.doi.org/10.1016/j.nima.2017.07.063

[7] C. Richter *et al.*, "First clinical application of a prompt gamma based in vivo proton range verification system," *Radiotherapy and Oncology*, vol. 118, no. 2, pp. 232–237, 2016. [Online]. Available: http://dx.doi.org/10.1016/j.radonc.2016.01.004

[8] G. Battistoni *et al.*, "Measurement of charged particle yields from therapeutic beams in view of the design of an innovative hadrontherapy dose monitor," *Journal of Instrumentation*, vol. 10, no. 2, 2015.

[9] A. C. Kraan, "Range Verification Methods in Particle Therapy: Underlying Physics and Monte Carlo Modeling," *Frontiers in Oncology*, vol. 5, no. July, pp. 1–27, 2015. [Online]. Available: http://journal.frontiersin.org/Article/10.3389/fonc.2015.00150/abstract

[10] G. Traini, I. Mattei, G. Battistoni, M. Bisogni, M. De Simoni, Y. Dong, A. Embriaco, M. Fischetti, M. Magi, C. Mancini-Terracciano *et al.*, "Review and performance of the dose profiler, a particle therapy treatments online monitor," *Physica Medica*, vol. 65, pp. 84–93, 2019.

[11] Y. Yu, Z. Li, D. Zhang, L. Xing, and H. Peng, "Simulation studies of time reversal-based protoacoustic reconstruction for range and dose verification in proton therapy," *Medical physics*, 2019.

[12] P. Moskal, B. Jasińska, E. Ł. Stepień, and S. D. Bass, "Positronium in medicine and biology," *Nature Reviews Physics*, p. 1, 2019.

[13] D. Kamińska *et al.*, "A feasibility study of ortho-positronium decays measurement with the J-PET scanner based on plastic scintillators," *Eur. Phys. J. C*, vol. 76, p. 445, 2016.

[14] P. Moskal, N. Krawczyk, B. Hiesmayr *et al.*, "Feasibility studies of the polarization of photons beyond the optical wavelength regime with the J-PET detector," *Eur. Phys. J. C*, vol. 78, p. 970, 2018.

[15] B. C. Hiesmayr and P. Moskal, "Witnessing entanglement in compton scattering processes via mutually unbiased bases," *Scientific reports*, vol. 9, 2019.

[16] B. Hiesmayr and P. Moskal, "Genuine multipartite entanglement in the 3-photon decay of positronium," *Scientific Reports*, vol. 7, p. 15349, 2017.

[17] L. Raczyński *et al.*, "Calculation of the time resolution of the j-pet tomograph using kernel density estimation," *Phys. Med. Biol.*, vol. 62, no. 12, pp. 5076–5097, 2017.

[18] G. Korcyl, P. Białas, C. Curceanu, E. Czerwiński, K. Dulski, B. Flak, A. Gajos, B. Głowacz, M. Gorgol, B. Hiesmayr *et al.*, "Evaluation of single-chip, real-time tomographic data processing on fpga soc devices," *IEEE transactions on medical imaging*, vol. 37, no. 11, pp. 2526–2535, 2018.

[19] M. Palka *et al.*, "Multichannel fpga based mvt system for high precision time (20 ps rms) and charge measurement," *JINST*, vol. 12, p. P08001, 2017.

[20] P. Kowalski, W. Wiślicki, R. Shopa, L. Raczyński, K. Klimaszewski *et al.*, "Estimating the nema characteristics of the j-pet tomograph using the gate package," *Phys. Med. Biol.*, vol. 63, p. 165008, 2018.

[21] P. Moskal, O. Rundel *et al.*, "Time resolution of the plastic scintillator strips with matrix photomultiplier readout for J-PET tomograph," *Phys. Med. Biol.*, vol. 61, pp. 2025–2047, 2016.

[22] A. Rucinski, J. Baran, G. Battistoni, A. Chrostowska, M. Durante, J. Gajewski, M. Garbacz, K. Kisielewicz, N. Krah, V. Patera *et al.*, "Investigations on physical and biological range uncertainties in krakow proton beam therapy centre," *arXiv preprint arXiv:1910.11943*, 2019.

[23] S. Jan *et al.*, "Gate v6: a major enhancement of the gate simulation platform enabling modelling of ct and radiotherapy," *Physics in Medicine & Biology*, vol. 56, no. 4, p. 881, 2011.

[24] J. Allison, K. Amako, J. Apostolakis, P. Arce, M. Asai, T. Aso, E. Bagli, A. Bagulya, S. Banerjee, G. Barrand *et al.*, "Recent developments in geant4," *Nuclear Instruments and Methods in Physics Research Section A: Accelerators, Spectrometers, Detectors and Associated Equipment*, vol. 835, pp. 186–225, 2016.

[25] E. Almhagen, D. J. Boersma, H. Nyström, and A. Ahnesjö, "A beam model for focused proton pencil beams," *Physica Medica*, vol. 52, pp. 27–32, 2018.

[26] T. Merlin, S. Stute, D. Benoit, J. Bert, T. Carlier, C. Comtat, M. Filipovic, F. Lamare, and D. Visvikis, "Castor: a generic data organization and processing code framework for multi-modal and multi-dimensional tomographic reconstruction," *Physics in Medicine & Biology*, vol. 63, no. 18, p. 185005, 2018.